Korean J. Chem. Eng., 35(4), 853-858 (2018)
DOI: 10.1007/s11814-018-0003-2

pISSN: 0256-1115
eISSN: 1975-7220

Biosynthesized Au/TiO_2@SBA-15 catalysts for selective oxidation of cyclohexane with O_2

Fang Yao*, Lixin Xu*, Jili Luo, Xiao Li*, Yue An***, and Chao Wan*,†**

*College of Chemistry and Chemical Engineering, Anhui University of Technology, 59 Hudong Road, Ma'anshan 243002, China
**Petro China Huabei Oilfield Company Gas Storage Management Service, 15 Battle Road, Renqiu 062550, China
***College of Chemical and Biological Engineering, Zhejiang University, 38 Zheda Road, Hangzhou 310027, China
(*Received 21 November 2016 • accepted 5 April 2017*)

Abstract−A variety of TiO_2@SBA-15 supporters with various TiO_2 loadings were synthesized using a facile sol-gel method. Gold (Au)-based catalysts were prepared with an environmentally benign and economical bioreduction method via *Cacumen Platycladi* (CP) leaf extract and immobilized on various TiO_2@SBA-15 supporters with different TiO_2 loadings. The as-prepared biosynthesized Au catalysts were applied in the liquid-phase cyclohexane oxidation. The results showed that the Au nanoparticles were well-dispersed on TiO_2@SBA-15, and the Au existed as Au^0. These biosynthesized Au catalysts are promising for cyclohexane oxidation, achieving a turnover frequency up to 3,426 h^{-1} with a 14.1% cyclohexane conversion rate.

Keywords: Cyclohexane Oxidation, Biosynthesis, Nanocomposites, Au/TiO_2@SBA-15, Oxygen

INTRODUCTION

The selective oxidation of hydrocarbons has been one of the most important chemical processes for producing intermediates and fine chemicals in modern chemistry, especially for the manufacturing of alcohols and ketones [1,2]. Among the various methods of hydrocarbon oxidation, cyclohexane oxidation has attracted the most attention, given that its main product, KA oil (a mixture of cyclohexanone [K] and cyclohexanol [A]), is a crucial chemical intermediate for producing nylon-6 and nylon-6,6 polymers [3,4]. Recently, great efforts have been devoted to investigating potential catalysts for cyclohexane oxidation, including homogeneous and heterogeneous catalysts [5-8]. Shul'pin et al. [9-11] reported that the binuclear manganese(IV) complex $[Mn_2L_2O_3][PF_6]_2$ (L=1,4,7-trimethyl-1,4,7-triazacyclononane) catalyzes very efficiently the oxygenation of cyclohexane alkanes with H_2O_2 only if a carboxylic (acetic, oxalic) acid is present as a co-catalyst. The biomimetic H_2O_2/$(OC)_3Fe(\mu\text{-}PhS)_2Fe(CO)_3$/pyrazine-2-carboxylic acid (PCA)/pyridine system was also investigated. However, the use of a homogeneous catalyst is limited owing to drawbacks of pollution and lack of recyclability [5,6]. Therefore, the design and preparation of environmentally friendly and highly efficient heterogeneous catalysts with relatively high conversion and selectivity for cyclohexane oxidation remain significant challenges.

Several recent studies have investigated heterogeneous catalysts for cyclohexane oxidation [12-17]. In view of its highly effective atom utilization and low environmental impact, molecular oxygen (O_2) is considered to be the most economical and efficient oxidant for cyclohexane oxidation [18,19]. However, it is very difficult to control the selective oxidation of cyclohexane using O_2 as an oxidant to simultaneously achieve high conversion of cyclohexane and selectivity for KA oil, which can easily be further oxidized to produce deep-oxidation byproducts such as adipic acid [19]. Gold (Au) catalysts have been identified as one of the most promising candidates for cyclohexane oxidation, since O_2 can be activated to react with cyclohexane under mild conditions [20]. To date, Au catalysts supported on metal-organic frameworks [21], hydroxyapatite [22], mesoporous silica-based materials [23], and metal oxides [24] have been investigated for their applications in the oxidation of cyclohexane. Furthermore, Au nanoparticle (NP) catalysts demonstrated more stable activity when semi-conductive metal oxides (Fe_2O_3, NiO, and TiO_2) were used as a supporter [25]. Martins et al. [26,27] reported that gold was loaded by two different methods, double impregnation and sol immobilization, on the different above-mentioned carbon supports. The obtained materials were applied in the oxidation of cyclohexane to cyclohexanol and cyclohexanone. When reaction conditions include acetonitrile (3.0 mL), cyclohexane (5.0 mmol), r.t., under dinitrogen; 0.1-9.9 μmol of Au catalyst (2-200 mg of Au/carbon material), the amount up to $n(H_2O_2)/n(\text{catalyst})$ molar ratio of 2×10^4 leads to the maximum products TON values (e.g., 171). Other studies showed that Au NPs immobilized on TS-1 [28], Al_2O_3 [29], MCM-41 [30], and SBA-15 [31,32] had high activity for the oxidation of cyclohexane using O_2. In particular, SBA-15 exhibits several advantages over other materials, such as a larger pore volume, long-range ordered mesoporous channels, high specific surface area, and high pore wall thickness, which confer it with excellent hydrothermal and thermal stability as well as enhanced acid-base tolerance [33]. Extensive studies have been conducted to investigate the metallic NPs and TiO_2 supported on SBA-15 in desulfurization and photocatalytic reactions; however, there is less information on the effects of noble metal NPs loaded on TiO_2-incorporated silica mesoporous materials for cyclo-

†To whom correspondence should be addressed.
E-mail: wanchao1219@hotmail.com

hexane oxidation.

The biosynthesis of metallic NPs using various plant extracts as reducing and stabilizing agents has been regarded as a green and effective method for producing nanocatalysts [34-41]. In some previous studies, poly(vinyl alcohol), polyvinyl pyrrolidone, and $NaBH_4$ were considered to be the optimal protecting and reducing agents to produce metallic NPs [42,43]. To date, biosynthesized metallic NP catalysts have been applied in many important industrial processes such as oxidation, epoxidation, and hydrogenation [34-38]. In this regard, we synthesized Au/TiO_2@SBA-15 with different TiO_2 loadings by a sol-immobilization technique through the immobilization of biosynthesized Au hydrosol onto TiO_2@SBA-15 supports, and obtained Au hydrosol by the reduction of chloroauric acid with *Cacumen Platycladi* (CP) leaf extract. The performance of Au/TiO_2@SBA-15 catalysts for the liquid-phase oxidation of cyclohexane to KA oil was investigated using O_2 as the oxidant. Furthermore, the influence of the Ti content on this performance was investigated. The catalysts were also characterized by X-ray diffraction (XRD), N_2 adsorption-desorption, transmission electron microscopy (TEM), and X-ray photoelectron spectroscopy (XPS).

EXPERIMENT SECTION

1. Materials

The template triblock copolymer poly(ethyleneoxide)-poly(propyleneoxide)-poly(ethyleneoxide) (EO_{20}-PO_{20}-EO_{20}, Pluronic P123, Mn~5800, ≥99%) was supplied by Sigma-Aldrich. $HAuCl_4 \cdot H_2O$ (AR), cyclohexane (AR), tetraethyl orthosilicate (TEOS, AR), tetrabutyl orthotitanate (TBOT, AR) and Triphenylphosphine (Ph_3P, AR) were purchased from Sinopharm Chemical Reagent Co. Ltd. Cacumen Platycladi (CP) was obtained from Ma'anshan Chuanyang drugstore. All Chemicals were used without any further treatment.

Mesoporous molecular sieves of SBA-15 were prepared according to the previous literature by Zhao et al. [44,45]. A typical procedure was as follows: 8 g of P123 was dissolved in 240 mL of 2 M of hydrochloric acid in a round-bottom flask and stirred at 313 K for 2 h. Then, 17 g tetraethyl orthosilicate (TEOS) was added slowly to the above mixture, stirred for another 24 h at 313 K and aged for 48 h at 373 K under static conditions. After aging, the resultant solid product was filtered, washed thoroughly with deionized water to reach neutral pH, dried at 363 K in an oven. Finally, the dried white powder was calcined in air atmosphere at 823 K for 6 h.

2. Synthesis of Au/TiO_2@SBA-15

The TiO_2@SBA-15 was prepared through post-synthesis method [46]. In a typical synthesis, 1 g of the as-synthesized SBA-15 was placed in dry ethanol (40 mL) under magnetic stirring. Then, a certain amount of tetrabutyl orthotitanate was added slowly to the above solution under stirring to obtain x wt% of TiO_2 on SBA-15 and the mixture was stirred continuously for another 5 h at 298 K. Next, 100 mL of (90% v/v) aqueous ethanol was added slowly and stirred for an hour. The acquired product was filtered and washed well with aqueous ethanol, dried and calcined at 823 K for 5 h. The synthesized TiO_2@SBA-15 support were named as x%TiO_2@SBA-15, where x represents the weight loading of TiO_2 (x=0, 1, 5, 10, 15).

To acquire the CP extract [47,48], 2 g screened Cacumen Platycladi (CP) leaf was added to 100 mL deionized water in a 250 mL shaker at 60 °C under stirring for 4 h. The mixture was then filtered to get filtrate (10 g/L) The concentration of this CP extract was denoted as 10 g/L and used for the subsequent preparation of Au NPs.

The Au-based catalyst were prepared by the sol-immobilization method using the as-prepared CP extract [48]. 0.1 g TiO_2@SBA-15 was impregnated with an aqueous $HAuCl_4$ solution (50 mL, 0.1 mmol/L) in a water bath at 90 °C for 1 h. Then 30 mL CP extract was slowly added to the solution and stirred for another 4 h. The suspension was filtered, washed and dried overnight at 50 °C in vacuum oven and calcined under N_2 at 873 K for 3 h. The loading of the gold metal was between 0.9 and 1.1 wt%. The synthesized catalysts were denoted as 1 wt% Au/x%TiO_2@SBA-15 (x=0, 1, 5, 10, 15).

3. Characterization

Powder X-Ray diffraction (XRD) patterns were conducted using a Japan Shimadzu XRD-6000 X-ray diffractometer with Cu-Kα radiation source (λ=0.154178 nm). Transmission electron microscopy (TEM) images were acquired using FEI Tecnai F20 at an acceleration voltage of 200 kV. The specific surface areas were measured using N_2 adsorption/desorption isotherms at 77 K with a Micromeritics ASAP 2020 analyzer after degassing in vacuum at 473 K for 4 h. X-ray photoelectron spectrometry (XPS) involved an Escalab 250Xi X-ray photoelectron spectrometer with an Al Kα source.

4. Cyclohexane Oxidation

The cyclohexane oxidation reaction was conducted in a 50 mL Teflon-lined stainless-steel autoclave under magnetic stirring. 10 mL of cyclohexane and 25 mg of catalyst were introduced into the reactor. The reactions were performed under the conditions of 423 K and pressures of 1.5 MPa controlled using O_2 under stirring at 800 rpm. The reactant was thoroughly cooled to room temperature after the termination of oxidation reaction, the catalyst was collected through centrifugation. Next, an excessive amount of triphenyphosphine (Ph_3P) was introduced to completely reduce the intermediate cyclohexylhydroperoxide (CHHP) into cyclohexanol. The products were measured using GC-9860 II (Shanghai Qiyang Information Technology Co., Ltd.) equipped with an HP-5 capillary column by a flame ionization detector using chlorobenzene as an internal standard substance. The side products were further confirmed by using Agilent 7890A-5975C gas chromatograph-mass spectrometry (GC-MS). The conversion of cyclohexane was expressed as follows:

$$X(\text{Cyclohexane}) = \frac{n(\text{Cyclohexane})_{initial} - n(\text{Cyclohexane})_{final}}{n(\text{Cyclohexane})_{initial}}$$

$n(\text{Cyclohexane})_{initial}$ and $n(\text{Cyclohexane})_{final}$ were denoted the molar content of cyclohexane in the initial reactant and the final product, respectively.

The selectivity to cyclohexanol (A) and cyclohexanone (K) was calculated, respectively, as follows:

$$S(\text{Cyclohexanol}) = \frac{n(\text{Cyclohexanol})}{n(\text{Cyclohexane})_{initial} - n(\text{Cyclohexane})_{final}}$$

$$S(\text{Cyclohexanone}) = \frac{n(\text{Cyclohexanone})}{n(\text{Cyclohexane})_{initial} - n(\text{Cyclohexane})_{final}}$$

$$S(\text{KA oil}) = \frac{n(\text{Cyclohexanol}) + n(\text{Cyclohexanone})}{n(\text{Cyclohexane})_{initial} - n(\text{Cyclohexane})_{final}}$$

n(Cyclohexanol) and n(Cyclohexanone) were denoted the molar content of cyclohexanol and cyclohexanone in the final product,

respectively. The selectivity of KA oil was the total of the selectivity to A and the selectivity to K.

RESULTS AND DISCUSSION

The catalytic performance of all catalysts tested is demonstrated in Table 1. The conversion of cyclohexane and the selectivity of KA oil were greatly improved with the introduction of TiO_2. The conversion of cyclohexane over Au/TiO_2@SBA-15 with various TiO_2 loadings increased by at least 3.2% compared to that over Au/SBA-15 in all cases. These results indicate that the addition of TiO_2 has a positive effect on enhancing the catalytic activity. The conversion of cyclohexane increased up to 14.1% over Au/10% TiO_2@SBA-15 with the selectivity of KA oil reaching 95.6%, and the turnover frequency reaching 3,426 h^{-1}.

As illustrated in Scheme 1, Au/TiO_2@SBA-15 is synthesized successfully by the biosynthesized method. The low-angle and wide-angle XRD patterns of SBA-15, Au/SBA-15, and Au/xTiO_2@SBA-15 with different Ti content are depicted in Fig. 1. All samples in the extreme low angle (2θ), shown in Fig. 1(A), demonstrate a sharp main diffraction peak and two weak peaks around 0.9°, 1.4°, and 1.6°, respectively. These peaks correspond to the facets of (100), (110), and (200) diffractions, suggesting the long-range ordered and well-defined hexagonal mesoporous structure of all these catalysts.

Table 1. Results of cyclohexane oxidation over different catalysts[a]

Catalysts	Conversion[a] (mol%)	Selectivity (mol%)			TOF (h^{-1})
		Cyclohexanol	Cyclohexanone	Others	
-	5	47.1	37.7	15.2	/
Au/SBA-15	8.9	44.1	45.2	10.7	2162
Au/1%TiO_2@SBA-15	12.1	44.5	45.4	10.1	2939
Au/5%TiO_2@SBA-15	13.4	45.1	45.8	9.1	3255
Au/10%TiO_2@SBA-15	14.1	47.2	48.4	4.4	3426
Au/15%TiO_2@SBA-15	12.9	45.3	45.7	9	3134

[a]Reaction conditions: 10 mL cyclohexane, 25 mg catalyst, initial P(O_2)=1.5 MPa, at 423 K for 3 h

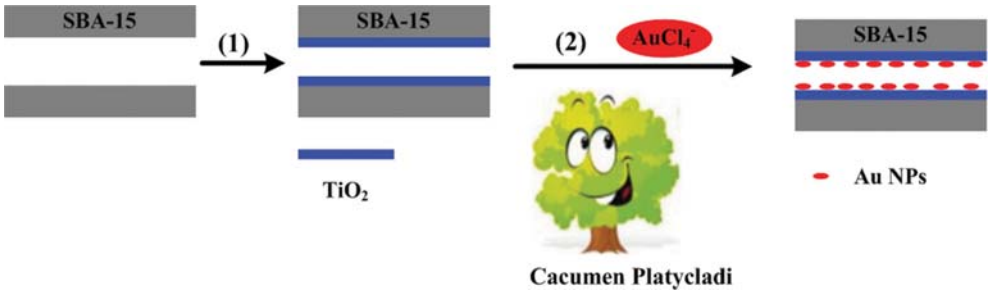

Scheme 1. Schematic illustration of the preparation of Au/TiO_2@ SBA-15 using the biosynthesized method.

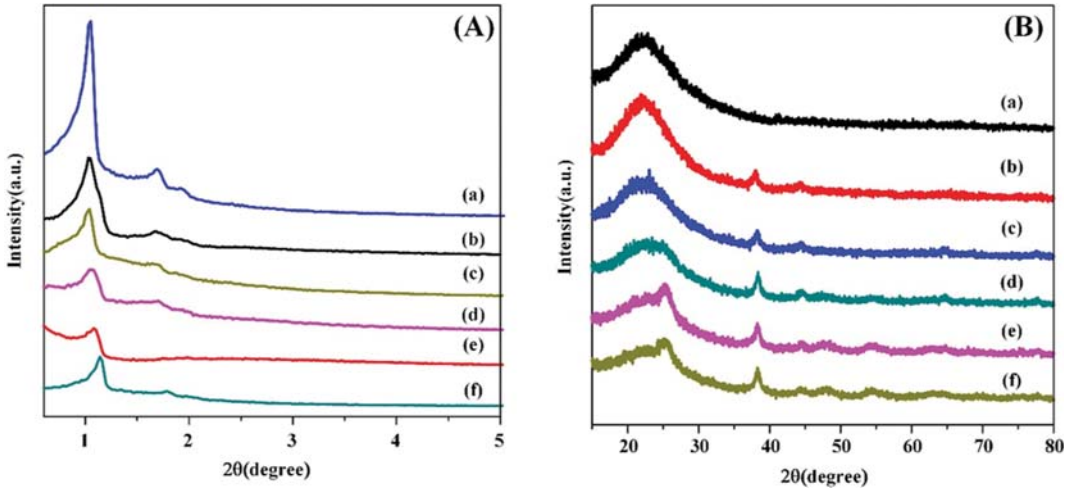

Fig. 1. (A) Low-angle and (B) wide-angle XRD patterns of the catalyst: (a) SBA-15; (b) Au/SBA-15; (c) Au/1%TiO_2@SBA-15; (d) Au/5%TiO_2@SBA-15; (e) Au/10%TiO_2@SBA-15; (f) Au/15%TiO_2@SBA-15.

The wide-angle diffraction patterns of all catalysts shown in Fig. 1(B) display a broad peak between 20° and 30°, reflecting the amorphous silica in the pore walls of SBA-15 [49]. For Au/TiO_2@SBA-15 with various TiO_2 loadings, TiO_2 particles are highly and uniformly dispersed on the SBA-15 surface, as reflected by the much lower intensity peaks at 2θ around 25.3°, 38.3°, 47.9°, 54.4°, and 62.5°, which can be ascribed to (101), (004), (200), (105), and (204). These XRD data are highly consistent with PDF card No. 21-1272 of the Joint Committee on Power Diffraction Standards [41,42]. In addition, Au NPs shows less intense peaks with 2θ values of 38.6°, 44.7°, 65°, and 78° (Fig. 1(b)-(f)), which can be attributed to the (111), (220), (200), and (311) planes of Au [50].

To further confirm the mesostructure of the catalysts, N_2 adsorption-desorption analyses were conducted, and the results are shown in Fig. 2. The isotherms of all catalysts indicated a type-IV isotherm pattern with H1 hysteresis loops, according to the IUPAC classification, which is typical for ordered mesoporous structures [49]. The structure parameters and the amount of supported metal in all the samples are listed in Table 2. Compared with the pure SBA-15, the Brunauer-Emmett-Teller (BET) surface areas of

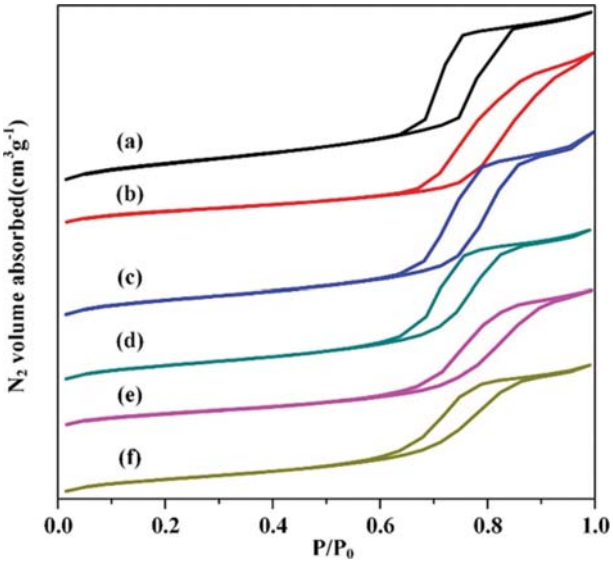

Fig. 2. N_2 adsorption-desorption isotherms of all catalysts: (a) SBA-15; (b) Au/SBA-15; (c) Au/1%TiO_2@SBA-15; (d) Au/5%TiO_2@SBA-15; (e) Au/10%TiO_2@SBA-15; (f) Au/15%TiO_2@SBA-15.

Table 2. Physico-chemical characterization of the catalysts

Catalysts	S_{BET} [a] (m^2g^{-1})	Au [b] (wt%)	TiO_2 [b] (wt%)
SBA-15	482	/	/
Au/SBA-15	331	0.9	/
Au/1%TiO_2@SBA-15	433	1.1	0.9
Au/5%TiO_2@SBA-15	423	1.1	5.1
Au/10%TiO_2@SBA-15	371	1.0	10.2
Au/15%TiO_2@SBA-15	344	1.1	14.8

[a]S_{BET}, BET surface areas calculated by the adsorption branch of N_2 isotherm

[b]The chemical compositions were determined by ICP-AES

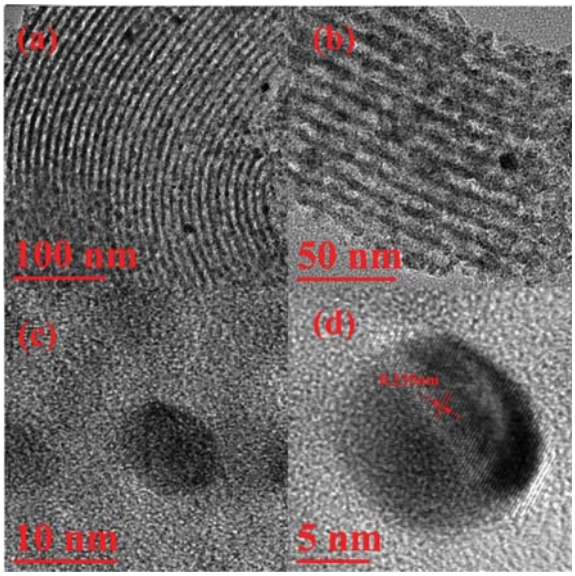

Fig. 3. TEM image of (a) (b) and (c) Au/10% TiO_2@SBA-15 with the different magnification and (d) HRTEM image of the Au/10% TiO_2@SBA-15.

the catalysts with different Ti content decreased with the increase of TiO_2 loading (Table 2), and the element composition was revealed. The reason for a decrease of the surface area for the catalysts might be attributed to occupation of TiO_2.

TEM images of the as-prepared Au/10%TiO_2@SBA-15 catalysts are displayed in Fig. 3. Well-resolved meso-channels are clearly observed in the Au/10%TiO_2@SBA-15 samples (Fig. 3(a), (b)), which indicate that the introduction of Au and Ti did not substantially destroy the regular ordered structure of the parent SBA-15, which is consistent with the low-angle XRD and BET results. Fig. 3(d) shows a high-resolution TEM image of the Au NPs; lattice fringes with a d-spacing of 0.235 nm are observed, which is in agreement with the Au(111) lattice planes [50,51]. This result confirms that the $HAuCl_4$ precursor was successfully transformed to metallic Au NPs with a face-centered cubic structure.

Fig. 4 shows the XPS spectra of the Au/10%TiO_2@SBA-15 catalysts. The binding energy at 84.7 eV can be attributed to Au $4f_{7/2}$, validating that the Au^{3+} species has transformed entirely into Au^0 (metallic) form in the synthetic procedure [51]. The binding energy of Ti $2p_{3/2}$ is centered at 458.8 eV for the Au/10%TiO_2@SBA-15 sample, and this peak position (933.6 eV) could be ascribed to Ti (IV) species on the surface of SBA-15. However, for the Au/10%TiO_2@SBA-15 sample, the binding energy for Ti 2p has shifted to a higher value, and that for Au 4f shifted to a lower value as compared to the core levels of pure Ti and Au, respectively. This result could be attributed to the interaction between Au and TiO_2.

This remarkable enhancement in catalytic activity suggests a synergy of the two factors. First, owing to the limit of the host material SBA-15, the growth of TiO_2 particles was restricted by the walls of the channels; thus, small and well-dispersed TiO_2 NPs were obtained. Second, the SBA-15 modified by TiO_2 preserved a high surface area and possessed strong surface adsorption ability to Au NPs. Therefore, the mesoporous channels and interaction

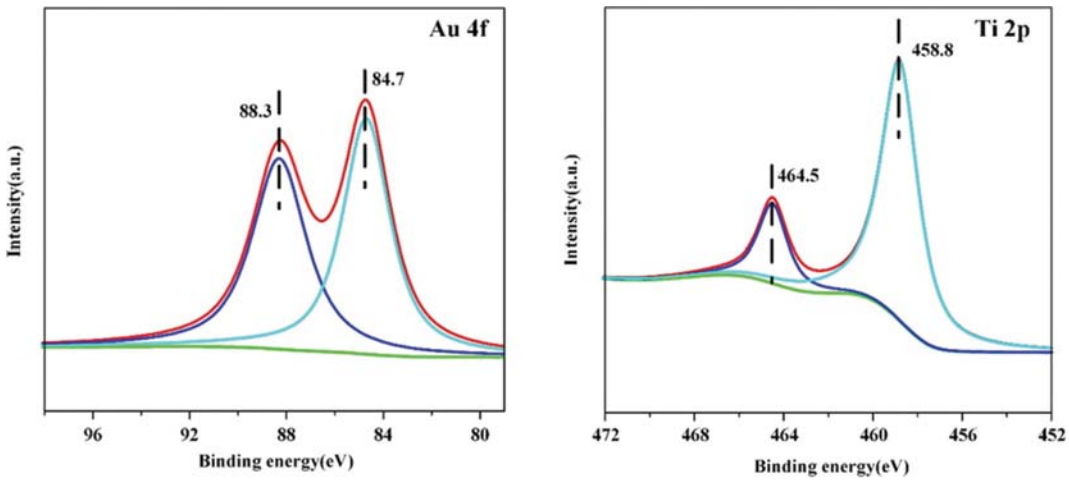

Fig. 4. XPS Au 4f and Ti 2p spectra for the Au/10% TiO_2@SBA-15.

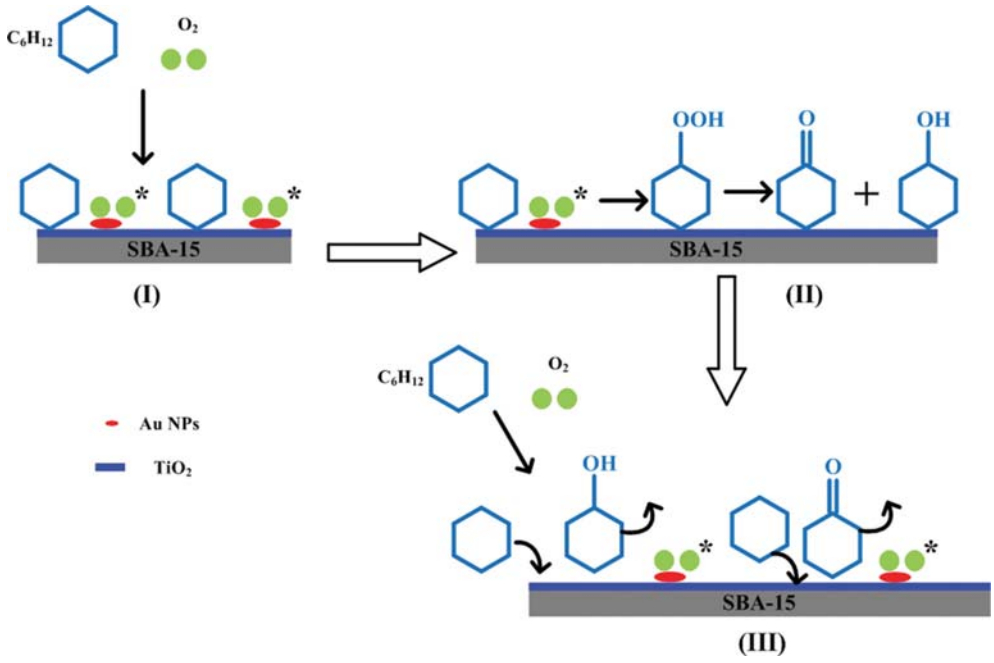

Scheme 2. Proposed mechanism of oxidation of cyclohexane on catalyst Au/TiO_2@ SBA-15.

between Au and TiO_2 in Au/TiO_2@SBA-15 contributed to the superior catalytic performance. As displayed in Scheme 2, cyclohexane molecules preferred the support surface, while oxygen was adsorbed and activated by Au nanoparticles (Step I). Reaction between dissociated oxygen and the adsorbed cyclohexane produced intermediate cyclohexyl hydroperoxide (CHHP), which decomposed to generate cyclohexanol and cyclohexanone adsorbed on the catalyst (Step II, III). These oxidation products can be further oxidized to byproducts, such as adipic acid and succinic acid, if they do not deviate from the surface promptly.

CONCLUSIONS

Au/TiO_2@SBA-15 catalysts with different TiO_2 loadings were successfully synthesized by a sol-immobilization technique through the reduction of chloroauric acid with CP leaf extract. The synergistic effect between Au and TiO_2, together with the mesoporous channels of the Au/TiO_2@SBA-15 catalysts could effectively enhance the catalytic performance of cyclohexane oxidation. To the best of our knowledge, this is the first report on the application of biosynthesized Au catalysts for the liquid-phase oxidation of cyclohexane to KA oil. Compared with Au catalysts prepared by traditional chemical methods, these catalysts are expected to accelerate the application of biosynthesis methods in industrial processes.

ACKNOWLEDGEMENTS

Financial support from National Natural Science Foundation of

China (21376005), Research Fund for Young Teachers of Anhui University of Technology (QZ201610) and the Scientific Research Foundation of Graduate School of Anhui University of Technology (2016012, 2016017) is gratefully appreciated.

REFERENCES

1. S. Bhattacharjee, Y. R. Lee and W.-S. Ahn, *Korean J. Chem. Eng.*, **34**(3), 701 (2017).
2. S. Y. Liu, Z. P. Liu and S. Kawi, *Korean J. Chem. Eng.*, **15**, 510 (1998).
3. J. G. Speight, Chemical and Process Design Handbook, McGraw-Hill, New York, 2185 (2002).
4. R. Zhao, Y. Q. Wang, Y. L. Guo, X. H. Liu, Z. G. Zhang, Y. S. Wang, W. C. Zhan and G. Z. Lu, *Green Chem.*, **8**, 459 (2006).
5. C. Santra, S. Shah, A. Mondal, J. K. Pandey, A. B. Panda, S. Maity and B. Chowdhury, *Micropor. Mesopor. Mater.*, **223**, 121 (2016).
6. N. F. Dummer, S. Bawaked, J. Hayward, R. Jenkins and G. J. Hutchings, *Catal. Today*, **154**, 2 (2010).
7. P. M. A. Machado, L. M. Lube, M. D. E. Tiradentes, C. Fernandes, C. A. Gomes, A. M. Stumbo, R. A. S. San Gil, L. C. Visentin, D. R. Sanchez, V. L. A. Frescura, J. S. A. Silva and A. Horn Jr., *Appl. Catal. A: Gen.*, **507**, 119 (2015).
8. G. Huang, L. Q. Mo, J. L. Cai, X. Cao, Y. Peng, Y. A. Guo and S. J. Wei, *Appl. Catal. B: Environ.*, **162**, 364 (2015).
9. G. B. Shul'pin, D. S. Nesterov, L. S. Shul'pina and A. J. L. Pombeiro, *Inorg. Chim. Acta*, **455**, 666 (2017).
10. G. B. Shul'pin, *Catalysts*, **6**, 50 (2016).
11. E. E. Karslyan, L. S. Shul'pina, Y. N. Kozlov, A. J. L. Pombeiro and G. B. Shul'pin, *Catal. Today*, **218-219**, 93 (2013).
12. P. F. Zhang, H. F. Lu, Y. Zhou, L. Zhang, Z. L. Wu, S. Z. Yang, H. L. Shi, Q. L. Zhu, Y. F. Chen and S. Dai, *Nat. Commun.*, **6**, 8446 (2015).
13. X. Liu, M. Contea, M. Sankar, Q. He, D. M. Murphy, D. Morgan, R. L. Jenkins, D. Knight, K. Whiston, C. J. Kiely and G. J. Hutchings, *Appl. Catal. A: Gen.*, **504**, 373 (2015).
14. P. P. Wu, P. Bai, Z. B. Lei, K. P. Loh and X. S. Zhao, *Micropor. Mesopor. Mater.*, **141**, 222 (2011).
15. K. Wu, B. S. Li, C. Y. Han and J. J. Liu, *Appl. Catal. A: Gen.*, **479**, 70 (2014).
16. S. Khare and P. Shrivastava, *J. Mol. Catal. A: Chem.*, **411**, 279 (2016).
17. H. Feng, J. W. Elam, J. A. Libera, M. J. Pellin and P. C. Stair, *J. Catal.*, **269**, 421 (2010).
18. J. L. Gu, Y. Huang, S. P. Elangovan, Y. S. Li, W. R. Zhao, I. Toshio, Y. Yamazaki and J. L. Shi, *J. Phys. Chem. C*, **115**, 21211 (2011).
19. Y. Fu, W. C. Zhan, Y. L. Guo, Y. Q. Wang, X. H. Liu, Y. Guo, Y. S. Wang and G. Z. Lu, *Micropor. Mesopor. Mater.*, **214**, 101 (2015).
20. P. P. Wu, P. Bai, Z. F. Yan and G. X. S. Zhao, *Sci. Rep.*, **6**, 18817 (2016).
21. Z. G. Sun, G. Li, L. P. Liu and H. O. Liu, *Catal. Commun.*, **27**, 200 (2012).
22. Y. Liu, H. Tsunoyama, T. Akita, S. Xie and T. Tsukuda, *ACS Catal.*, **1**, 2 (2011).
23. B. P. C. Hereijgers and B. M. Weckhuysen, *J. Catal.*, **270**, 16 (2010).
24. L. Li, W. Ji and C.-T. Au, *Prog. Chem.*, **21**, 1742 (2009).
25. M. Haruta, *Gold Bull.*, **37**, 27 (2004).
26. S. A. C. Carabineiro, L. M. D. R. S. Martins, M. Avalos-Borja, J. G. Buijnsters, A. J. L. Pombeiro and J. L. Figueiredo, *Appl. Catal. A: Gen.*, **467**, 279 (2013).
27. M. P. de Almeida, L. M. D. R. S. Martins, S. A. C. Carabineiro, T. Lauterbach, F. Rominger, A. S. K. Hashmi, A. J. L. Pombeiro and J. L. Figueiredo, *Catal. Sci. Technol.*, **3**, 305 (2013).
28. L.-Y. Ma, J.-C. Zhou and H. Zhao, *Chem. React. Eng. Technol.* (Chin.), **3**, 228 (2007).
29. L.-X. Xu, C.-H. He, M.-Q. Zhu and S. Fang, *Catal. Lett.*, **114**, 202 (2007).
30. G.-M. Lü, R. Zhao, G. Qian, Y.-X. Qi, X.-L. Wang and J.-S. Suo, *Catal. Lett.*, **97**, 115 (2004).
31. X. G. Duan, W. M. Liu, L. M. Yue, W. Fu, M. N. Ha, J. Li and G. Z. Lu, *Dalton Trans.*, **44**, 17381 (2015).
32. N. Yu, Y. Ding, A. Y. Lo, S. J. Huang, P. H. Wu, C. Liu, D. Yin, Z. Fu, D. Yin, C. T. Hung, Z. Lei and S. B. Liu, *Micropor. Mesopor. Mater.*, **143**, 426 (2011).
33. D. Y. Zhao, Q. S. Huo, J. L. Feng, B. F. Chmelka and G. D. Stucky, *J. Am. Chem. Soc.*, **120**, 6024 (1998).
34. J. L. Huang, L. Q. Lin, D. H. Sun, H. M. Chen, D. P. Yang and Q. B. Li, *Chem. Soc. Rev.*, **44**, 6330 (2015).
35. G. Ghodake and D. S. Lee, *Korean J. Chem. Eng.*, **28**, 2329 (2011).
36. G. W. Zhan, Y. L. Hong, V. T. Mbah, J. L. Huang, A. R. Ibrahim, M. M. Du and Q. B. Li, *Appl. Catal. A: Gen.*, **439**, 179 (2012).
37. M. M. Du, G. W. Zhan, X. Yang, H. X. Wang, W. S. Lin, Y. Zhou, J. Zhu, L. Lin, J. L. Huang, D. H. Sun, L. S. Jia and Q. B. Li, *J. Catal.*, **283**, 192 (2011).
38. Y. Q. Huang, Y. Ma, Y. W. Cheng, L. J. Wang and X. Li, *Appl. Catal. A: Gen.*, **495**, 124 (2015).
39. J. Annamalai and T. Nallamuthu, *Appl. Nanoscience*, **5**, 603 (2015).
40. J. L. Huang, Q. B. Li, D. H. Sun, Y. H. Lu, Y. B. Su, X. Yang, H. X. Wang, Y. P. Wang, W. Y. Shao and N. He, *Nanotechnology*, **18**, 105104 (2007).
41. A. M. Abdelghany, E. M. Abdelrazek, S. I. Badr, M. S. Abdel-Aziz and M. A. Morsi, *J. Saudi Chemical Society* (2015), DOI:10.1016/j.jscs.2015.10.002.
42. Z. H. Wang, H. F. Fu, D. M. Han and F. B. Gu, *J. Mater. Chem. A*, **2**, 20374 (2014).
43. Y. Zhao, J. A. Baeza, N. K. Rao, L. Calvo, M. A. Gilarranz, Y. D. Li and L. Lefferts, *J. Catal.*, **318**, 162 (2014).
44. D. Y. Zhao, J. L. Feng, Q. S. Huo, N. Melosh, G. H. Fredrickson, B. F. Chmelka and G. D. Stucky, *Science*, **279**, 548 (1998).
45. J. Yang, J. Zhang, L. Zhu, S. Chen, Y. Zhang, Y. Tang, Y. Zhu and Y. Li, *J. Hazard. Mater. B*, **137**, 952 (2006).
46. C. L. Peza-Ledesma, L. Escamilla-Perea, R. Nava, B. Pawelec and J. L. G. Fierro, *Appl. Catal. A: Gen.*, **375**, 37 (2010).
47. Y. Q. Huang, Y. Ma, Y. W. Cheng, L. J. Wang and X. Li, *Catal. Commun.*, **72**, 20 (2015).
48. Y. L. Hong, X. L. Jing, J. L. Huang, D. H. Sun, T. Odoom-Wubah, F. Yang, M. M. Du and Q. B. Li, *ACS Sustainable Chem. Eng.*, **2**, 1752 (2014).
49. X. H. Li, W. L. Zheng, H. Y. Pan, Y. Yu, L. Chen and P. Wu, *J. Catal.*, **300**, 9 (2013).
50. J. C. Zhou, X. F. Yang, Y. Q. Wang and W. J. Chen, *Catal. Commun.*, **46**, 228 (2014).
51. Y. Chen, J. Y. Wang, W. Z. Li and M. T. Ju, *Mater. Lett.*, **159**, 131 (2015).